

Powerful CMD: a tool for color-magnitude diagram studies

Zhong-Mu Li¹, Cai-Yan Mao¹, Qi-Ping Luo¹, Zhou Fan², Wen-Chang Zhao¹, Li Chen¹, Ru-Xi Li¹ and Jian-Po Guo³

¹ Institute for Astronomy and History of Science and Technology, Dali University, Dali 671003, China; zhongmuli@126.com

² Key Laboratory for Optical Astronomy, National Astronomical Observatories, Chinese Academy of Sciences, Beijing 100012, China

³ College of Science and Technology, Puer University, Puer 665000, China

Received 2016 October 27; accepted 2017 March 21

Abstract We present a new tool for color-magnitude diagram (CMD) studies, *Powerful CMD*. This tool is built based on the advanced stellar population synthesis (ASPS) model, in which single stars, binary stars, rotating stars and star formation history have been taken into account. Via *Powerful CMD*, the distance modulus, color excess, metallicity, age, binary fraction, rotating star fraction and star formation history of star clusters can be determined simultaneously from observed CMDs. The new tool is tested via both simulated and real star clusters. Five parameters of clusters NGC 6362, NGC 6652, NGC 6838 and M67 are determined and compared to other works. It is shown that this tool is useful for CMD studies, in particular for those utilizing data from the *Hubble Space Telescope (HST)*. Moreover, we find that inclusion of binaries in theoretical stellar population models may lead to smaller color excess compared to the case of single-star population models.

Key words: (stars:) Hertzsprung-Russell and C-M diagrams — (Galaxy:) globular clusters: general — galaxies: clusters: general

1 INTRODUCTION

A color-magnitude diagram (CMD) is the observed counterpart of the Hertzsprung-Russell diagram. It shows the distribution of stars in the magnitude versus color plane. CMDs are of key importance for studies of star clusters. Many astrophysical properties, e.g., distance modulus, color excess, metallicity, age, binary fraction and star formation history, can be determined from CMDs. Such results can be widely used for studying the evolution of stars, star clusters and galaxies. The age of the universe can also be constrained by the age of the oldest globular clusters, which can be derived from CMDs. The CMD of a star cluster can be obtained by observing stars within the cluster in two passbands. There have been many observations with the goal of constructing CMDs of star clusters. Both ground-based and space-based telescopes have been used. In particular, a quantity of high-quality CMDs has been obtained by the *Hubble Space Telescope (HST)*. This makes it possible for us

to study star clusters in detail via CMDs. One can read many papers about CMD studies, e.g., Fusi Pecci et al. (1996), Olsen et al. (1998), Mieske et al. (2006), Mackey & Broby Nielsen (2007), VandenBerg et al. (2013), Yang et al. (2013), Li et al. (2012a, 2015), Brandt & Huang (2015) and Niederhofer et al. (2016).

One method that is widely used to study star clusters is based on the comparison between observed and synthetic CMDs. In most works, synthetic CMDs are described by some isochrones (distribution of a population of stars with the same metallicity and age but varying masses). The comparison of observed and theoretical CMDs can be simply done *by eye*, but this is usually for a small set of isochrones. This method is unsuitable for studying a large number of clusters. It is also not suitable for some detailed studies, which need numerous isochrones. Therefore, many works tried to fit CMDs via some statistical methods, for example: (1) Bayesian method; (2) χ^2 method; (3) τ^2 method; (4) likelihood statistic.

The Bayesian method was used by e.g., von Hippel et al. (2006) and De Gennaro et al. (2009). This technique applies information from data and from our prior knowledge to obtain posterior distributions on the parameters (e.g., metallicity, age and initial mass of cluster stars) of stellar population models. The χ^2 method was used by e.g., Harris & Zaritsky (2001), Kerber & Santiago (2005) and Cignoni & Shore (2006). This method is good for the ideal case with single Gaussian uncertainties but it has been widely implemented in similar cases. The τ^2 method was utilized by Naylor & Jeffries (2006) and Da Rio et al. (2010). A parameter, $\tau^2 = -2 \ln P$ (where P is probability), is used to identify the best-fit models. The distribution of τ^2 is different from that of χ^2 when uncertainties are small, but the two goodness of fit parameters have similar distributions for a case with large uncertainty. A likelihood statistic was used by Kerber et al. (2002), and the χ_e^2 method was used by e.g., Dolphin (2002). The likelihood L is given by $L = \prod P_i$, where P_i is the model probability function evaluated at the CMD position of the i th star. Such methods are much more quantitative than the *by eye* method, and they obviously improve the reliability of CMD fitting. A limitation of the previous works is that they are based on some classical stellar population synthesis models, and some of them only consider part of a CMD, e.g., the main sequence, rather than the whole CMD. In addition, no tool is able to simultaneously determine cluster properties including e.g., binary fraction, rotating star fraction and star formation history. This makes it difficult to get a comprehensive understanding about star clusters from CMDs.

This work introduces a tool, i.e., *Powerful CMD*, produced by Dr. Zhongmu Li, which is aiming to determine the distance modulus, color excess, metallicity, age, binary fraction and star formation history from CMDs. It can also be used for building the CMDs of various kinds of stellar populations. The working principle, tests and application of the new tool are presented in this work.

This paper is organized as follows. In Section 2, we briefly introduce the stellar population model used by *Powerful CMD*. In Section 3, we introduce how *Powerful CMD* builds synthetic CMDs and finds the best-fit models. Next, in Section 4, we present some tests of the new tool. In Section 5, we apply the tool to a few star clusters. Finally, we give our discussions and conclusions in Section 6.

2 STELLAR POPULATION MODEL

Powerful CMD works based on the advanced stellar population synthesis (ASPS) model of Dr. Zhongmu Li. The ASPS model was developed from the rapid stellar pop-

ulation synthesis model (RPS) (Li & Han 2008a,b; Li et al. 2010; Li 2011; Li et al. 2012b, 2013, 2015). A feature of ASPS is taking the effects of binary stars and rotating stars into account (Li et al. 2012a, 2015, 2016). The current version of ASPS incorporates the initial mass function (IMF) of Salpeter (1955) (Salpeter IMF), eight metallicities (0.0001, 0.0003, 0.001, 0.004, 0.008, 0.01, 0.02 and 0.03), 151 ages (0–15 Gyr with an interval of 0.1 Gyr) and seven rotating star fractions (0, 0.1, 0.3, 0.5, 0.7 and 1.0 for stars following the rotation rate distribution of Royer et al. (2007), and a Gaussian distribution with mean and deviation of 0.7 and 0.1 respectively for all stars). Although there is still some uncertainty in the IMF for stars less massive than the Sun, this aspect does not obviously affect the results, because bright stars (i.e., massive stars at zero age) are usually targeted for CMD studies. Results from the Geneva code are included by considering stellar rotation in ASPS, and our results are consistent with some recent works, e.g., Brandt & Huang (2015), D’Antona et al. (2015) and Niederhofer et al. (2015). Because the Geneva models do not include low-mass (<1.7 solar mass) rotating stars, rotation is not considered by ASPS for star clusters older than about 2 Gyr. In fact, rotation affects old clusters (>2 Gyr) much less than young ones, as such clusters are dominated by low-mass and slowly-rotating stars.

The basic stellar population models of ASPS take a binary fraction of 50%. Note that binaries here mean those with orbital period less than 100 yr. They are different from interacting binaries. Therefore, the binary fraction in this paper is usually larger than in other works. Because every single and binary star in basic models can be removed, binary fraction can be changed to any value between 0 and 1 in studies. The star sample of ASPS is generated by a Monte Carlo technique following the Salpeter IMF at zero age, then all stars are evolved to present day using the rapid stellar evolution code of Hurley & Tout (1998) and Hurley et al. (2002). The effect of rotation on the evolution of stars is calculated using the results of Georgy et al. (2013), via taking various rotation rate distributions, i.e., the above-mentioned seven rotating star fractions. Readers are kindly invited to read another paper, Li et al. (2016), to learn more details about ASPS.

3 SYNTHETIC CMDS AND CMD FITTING

3.1 Synthetic CMDs

The ASPS model only supplies some basic stellar populations with 50% binaries, but we can change the binary fraction of a stellar population in the synthesis of CMDs

because the binarity (binary or single) of every star has been marked. This is easily achieved by removing some random binaries or single stars from the basic models. Moreover, stellar population models with various rotating star fractions can be chosen from the basic models of ASPs. The CMDs of simple stellar populations (SSPs) with a fraction of binaries and a fraction of rotating stars can be built in this way (e.g., panels (a), (b), (e) and (f) of Fig. 1). When we build the CMDs of composite stellar populations (CSPs), *Powerful CMD* puts a few SSPs together. Because the stars of most studied star clusters ($\sim 80\%$) have no obvious metallicity difference, we assume that a CSP consists of stars with the same metallicity but various ages. Here we do not take into account chemical evolution, because observations did not show obvious metallicity difference for the stars from a not too old cluster. The number of stars for each SSP is assigned according to a chosen star formation history, for clarity. In this way, the intrinsic CMDs of SSPs and CSPs are built.

Figure 1 shows some examples. Each panel presents the CMD of a kind of stellar population. In detail, panels (a)–(d) contain no rotating stars, while the others include a rotating star fraction. Panels (a), (c), (e) and (g) contain no binary stars, while the others contain some binaries. Panels (c), (d), (g) and (h) are for CSPs and the others for SSPs. The model inputs of these example stellar populations are listed in Table 1.

Table 1 Input parameters for eight simulated star clusters in Fig. 1. Z , f_b and f_{rot} denote metallicity, binary fraction and rotating star fraction, respectively.

No.	Z	Age (Gyr)	f_b	f_{rot}
a	0.01	0.5	0	0
b	0.001	1.5	0.5	0
c	0.004	0.9, 1.0, 1.1, 1.2	0	0
d	0.02	0.6, 0.7, 0.8	0.5	0
e	0.008	1.0	0	0.5
f	0.008	1.0	0.5	0.5
g	0.008	0.9, 1.0, 1.1, 1.2, 1.3	0	1.0
h	0.008	0.9, 1.0	0.7	1.0

In fact, the observed CMDs are obviously affected by distance, color excess and uncertainties in magnitudes and colors. This makes observed CMDs different from the intrinsic CMDs of theoretical stellar populations. Therefore, it is necessary to include this effect in synthetic CMDs. In detail, the magnitudes of stars are moved toward the less luminous direction by adding a distance modulus, and their colors are shifted toward the redder direction by adding a color excess. Because color

excess corresponds to the faintness of stars, we need to correct the distance modulus after getting the results. A correlation between color excess and magnitude change is needed for this operation, which depends on the dust distribution model of the Milky Way.

A difficulty in modeling CMDs accurately is correctly taking into account the observational uncertainties of magnitudes. Such uncertainties are caused mainly by equipment implemented for observations, software and methods utilized for dealing with data (i.e., photometry process) and random errors. The uncertainties caused by equipment and the photometry process dominate observational uncertainties. Usually, uncertainties caused by equipment are reported, but those caused by the photometry process are not so clear. In order to quantify uncertainties due to the photometry process, we can perform some artificial star tests (ASTs) (e.g., Sandquist et al. 1996, Harris & Zaritsky 2001, Anderson et al. 2008 and Rubele et al. 2010). Some images consisting of many artificial stars with known magnitudes and colors are constructed and then processed with photometry software to measure their magnitudes. The magnitude uncertainties (AST uncertainties) caused by the photometry process are derived by comparing the input and measured magnitudes. In addition, the star completeness in any CMD region is given by comparing the input and measured star fractions. Although ASTs can account for only a part of the observational errors, some tests (e.g., Rubele et al. 2010) have shown that the AST technique can be used for some CMD works.

Figure 2 shows the uncertainty versus magnitude relations of stars in two simulated star clusters (S1 and S6). Such relations will be used for adding AST uncertainties to intrinsic CMDs of stellar populations. When such uncertainties are considered, the CMDs of stellar populations usually become significantly scattered and seem closer to the observed ones. In the case that uncertainties due to the photometry process are much larger than those caused by equipment, we can use the results of ASTs as the final observational uncertainties. However, we should note that real observational errors are larger than AST ones. For example, differential reddening and PSF variations also contribute to the observational errors (Milone et al. 2009, 2012). We suggest taking these errors into account if possible. After including observational uncertainties, CMDs in Figure 1 change to the case shown in Figure 3. Note that many other methods can be used for estimating the observational uncertainties, so one can choose his/her own methods.

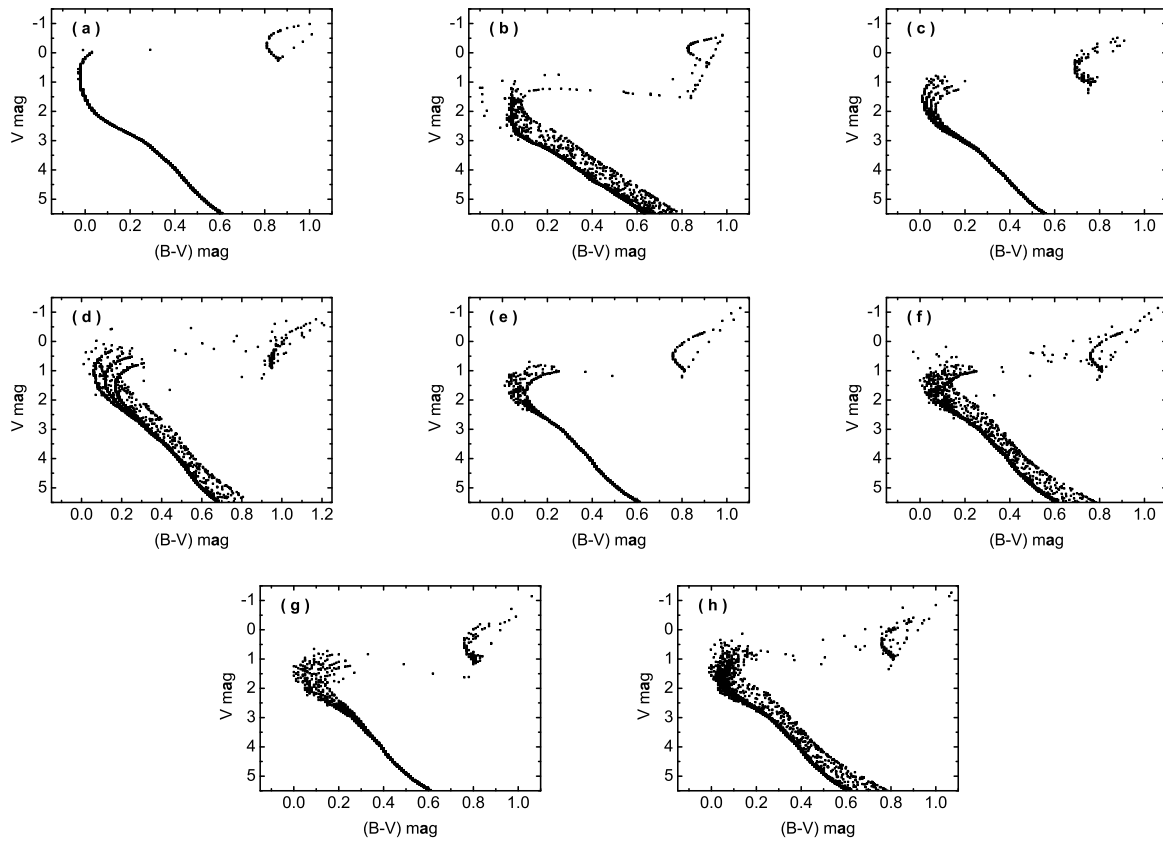


Fig. 1 Examples of intrinsic CMDs for various stellar populations. All CMDs are compiled via *Powerful CMD*. Model inputs are provided in Table 1.

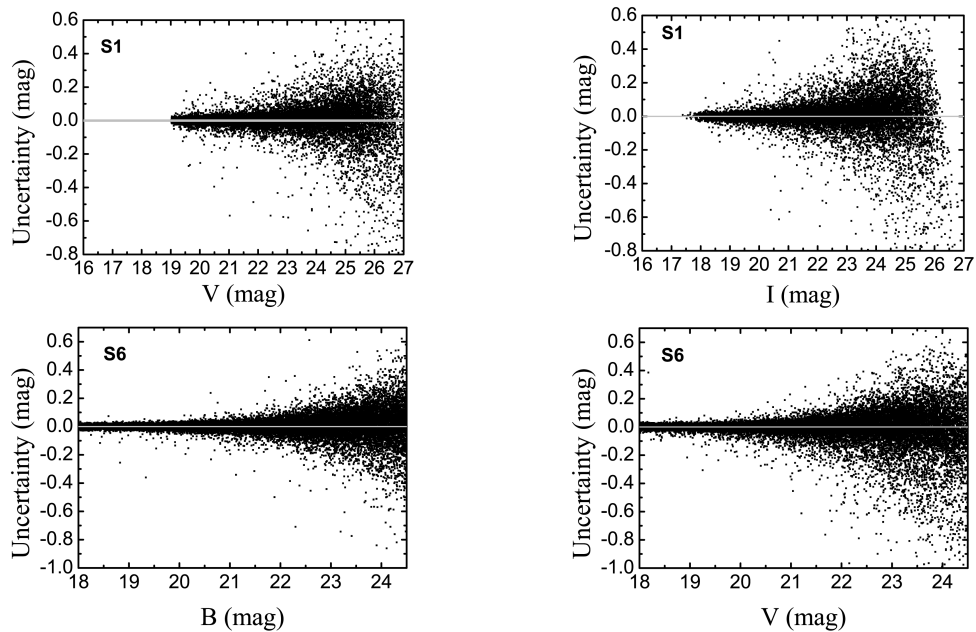


Fig. 2 Magnitude uncertainty as a function of observed magnitude for two simulated star clusters. The uncertainties are estimated via ASTs, and the errors relating to observational equipment are not taken into account because they are usually much smaller.

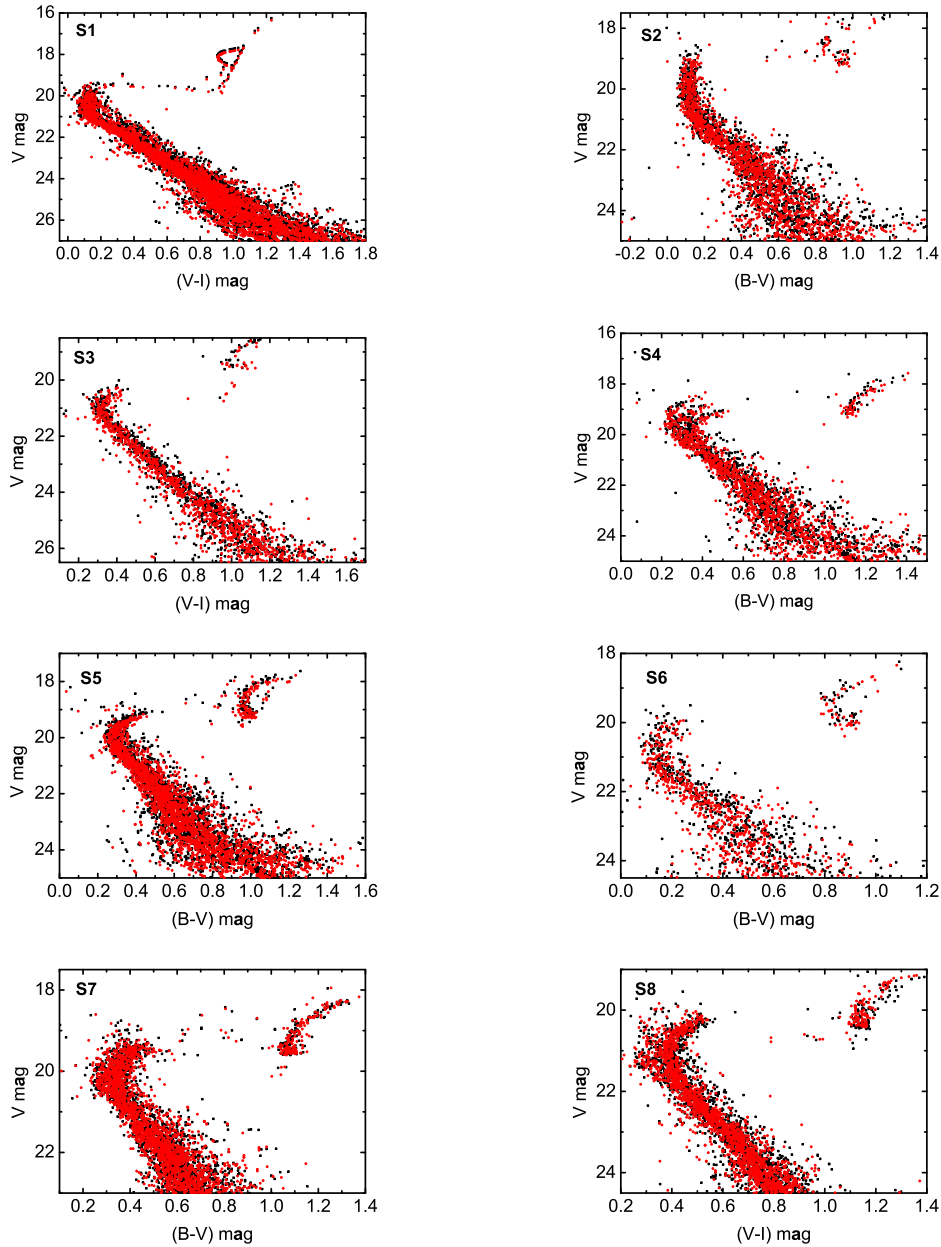


Fig. 3 Example CMDs (*black*) of simulated stellar populations and their best-fit CMDs (*red*). The best-fit CMDs are found by *Powerful CMD*.

3.2 CMD Fitting

In order to make CMD fitting more convenient and effective, *Powerful CMD* divides a CMD into many cells by taking fixed color and magnitude intervals and counts the stars in each cell. Then it fits the Hess diagrams (Hess 1924) instead of the original CMDs to find the best-fit parameters of star clusters. In the standard case, a CMD plane is divided into 1500 cells, including 50 color bins and 30 magnitude bins, but these values can be changed. It is suggested to test the effect of bin numbers on the

result. Our test shows that this selection is able to reproduce most of the input CMDs. One can also implement fixed intervals for color and magnitude in the fitting. In principle, if synthetic CMDs are well built, the result will not be affected too much by the color and magnitude bins when they are larger than about 30. The star fractions of observed and theoretical CMDs in the same cell are denoted by f_{ob} and f_{th} respectively for comparison.

Although a few statistics can be used for finding the best-fit models, they all have both advantages and disad-

vantages. Thereby, *Powerful CMD* uses three statistics to identify the best-fit model. Users can choose the statistic for CMD fitting. The three statistics in the current version include the widely used χ^2 , effective χ_e^2 (Bertelli et al. 2003), and weighted average difference (WAD, Li et al. 2015). Note that the χ_e^2 statistic is appropriate for dealing with Poisson-distributed data. In Li et al. (2015), we compared WAD with χ^2 and χ_e^2 statistics. It was shown that WAD is a good indicator for determining the best-fit parameters of star clusters, and it gives results that are similar to χ^2 . In detail, WAD, χ^2 and χ_e^2 are calculated via Equations (1)–(4).

$$\text{WAD} = \frac{\sum[\omega_i |f_{\text{ob}} - f_{\text{th}}|]}{\sum \omega_i}, \quad (1)$$

where ω_i is the weight of the i th cell, and f_{ob} and f_{th} are star fractions of observed and theoretical CMDs in the same cell respectively. Both f_{ob} and f_{th} are between 0 and 1. ω_i is greater than 0, and it is calculated as

$$\omega_i = \frac{1}{|1 - C_i|}, \quad (2)$$

where C_i (<1) is the completeness of the i_{th} cell, and it can be estimated via ASTs (see Li et al. 2015). Here $|1 - C_i|$ gives the uncertainty of star fraction in the i_{th} cell.

$$\chi^2 = \sum \frac{(f_{\text{ob}} - f_{\text{th}})^2}{(1 - C_i)^2}, \quad (3)$$

and

$$\chi_e^2 = 2\sum[(f_{\text{ob}} - f_{\text{th}}) + f_{\text{th}} \log(f_{\text{th}}/f_{\text{ob}})]. \quad (4)$$

CMD fitting can be completed automatically by *Powerful CMD*, when the observational data and control file have been prepared. In the control file, one needs to set the number of stars in theoretical models, color for fitting, considering observational errors and star incompleteness or not, CMD range for fitting, and the range of star formation mode. The ranges and steps for distance modulus, color excess, metallicity, age, age spread, binary fraction and rotating star fraction also need to be given in this file. This makes the tool user friendly.

Powerful CMD is possibly able to be applied in some current researches, e.g., the extended main-sequence turn off of star clusters with age of 100–2000 Myr, which has attracted much attention, but the associated mechanism is still not clear. Both a spread in age (e.g., Mackey et al. 2008; Milone et al. 2009) and a spread in stellar rotation rate (e.g., D’Antona et al. 2015) can possibly explain these observations. With the aim of finding whether *Powerful CMD* can be used for disentangling the effects of spread in age and spread in rotation rate of stars, we

did a test. We found that *Powerful CMD* can partially disentangle the degeneracy between spread in age and spread in rotation rate. If extended star clusters or multiple red clumps exist, *Powerful CMD* usually prefers age spread as the reason for extended turn-off, because such a special red clump structure is possibly not formed from rotation, as rotation of stars becomes much slower when they leave the main sequence and lose a lot of angular momentum. Similarly, for star clusters younger than 0.5 Gyr, *Powerful CMD* usually reports age spread because rotation slightly contributes to extended turn-off (Li et al. 2015). For other clusters, *Powerful CMD* cannot provide a reliable conclusion due to the extended turn off, although a best-fit model can be given. Note that the results depend on the stellar population model.

4 TEST OF THE NEW TOOL

4.1 Building CMDs of Various Stellar Populations

A function of *Powerful CMD* is to generate CMDs based on different stellar population assumptions. Different metallicities, ages, binary fractions, rotating star fractions, star formation histories, distance moduli and color excesses can be taken, and CMDs can be generated quickly (about decades of seconds for a few thousand stars but it depends on the computer).

Figure 1 provided some examples without observational uncertainties, so we test the CMD building function by taking color and magnitude uncertainties into account here. As examples, Figure 3 shows the CMDs of eight simulated star clusters (black points). The model inputs are listed in Tables 2 and 3, while the corresponding magnitude uncertainties of stars in two clusters can be seen in Figure 2. This demonstrates *Powerful CMD* has the ability to build the CMDs of various stellar populations, which is helpful for many studies of star clusters and galaxies.

4.2 Fitting CMDs of Stellar Populations

The WAD method was tested in a previous work (Li et al. 2015) and its reliability has been shown, but this method cannot yield a constraint on the uncertainties of cluster parameters, because we do not know the distribution of WAD values. Thus we choose χ^2 as the goodness of fit indicator and test *Powerful CMD* in this paper. The results show that this method can recover most cluster parameters, when we use some artificial star clusters to test *Powerful CMD*.

Figure 4 shows the process (only a few example steps) of CMD fitting. We observe that this code is able

Table 2 Input and Fitted Parameters for Eight Simulated Star Clusters

No.	$(m - M)_{\text{in}}$ [mag]	$(m - M)_{\text{fit}}$ [mag]	Range [mag]	CE_{in} [mag]	CE_{fit} [mag]	Range [mag]	Z_{input}	Z_{fit}	Range
S1	18.40	18.37	18.28–18.58	0.08	0.08	0.04–0.12	0.0010	0.0010	0.0003–0.0010
S2	19.00	18.93	18.88–19.18	0.16	0.15	0.12–0.20	0.0040	0.0040	0.0010–0.0080
S3	19.00	18.98	18.98–19.18	0.16	0.15	0.11–0.19	0.0040	0.0040	0.0040–0.0080
S4	18.50	18.48	18.48–18.68	0.18	0.18	0.12–0.24	0.0200	0.0200	0.0100–0.0300
S5	18.30	18.30	18.28–18.46	0.14	0.14	0.08–0.20	0.0100	0.0100	0.0080–0.0200
S6	19.20	19.24	19.18–19.37	0.13	0.12	0.09–0.17	0.0040	0.0040	0.0010–0.0080
S7	18.40	18.40	18.30–18.50	0.08	0.08	0.00–0.18	0.0080	0.0080	0.0080
S8	19.50	19.44	19.40–19.60	0.15	0.14	0.10–0.20	0.0080	0.0080	0.0080

Notes: “CE” means color excess. Subscripts “in” and “fit” denote input and fitted parameters respectively. Parameter ranges are 1σ ranges.

Table 3 Similar to Table 2, but for Other Parameters

No.	Age_{in} [Gyr]	Age_{fit} [Gyr]	Range [Gyr]	F_{bin}	F_{bin}	Range	$N_{\text{sf in}}$	$N_{\text{sf fit}}$	Range	mod_{in}	mod_{fit}	$F_{\text{r in}}$	$F_{\text{r fit}}$
S1	1.5	1.5	1.2–1.8	0.5	0.4	0.2–0.8	1	1	1–3	1	1	0	0
S2	0.5	0.5	0.2–0.8	0.7	0.8	0.4–1.0	2	3	1–3	1	2	0	0
S3	1.3	1.3	0.9–1.8	0.0	0.2	0.0–0.3	2	3	1–3	1	2	0	0
S4	0.6	0.6	0.3–0.9	0.5	0.7	0.2–0.8	3	3	1–3	1	1	0	0
S5	1.0	1.0	0.8–1.1	0.5	0.4	0.3–0.8	1	1	1–1	1	1	0	0
S6	0.8	0.9	0.5–1.1	0.0	0.0	0.0–0.0	4	3	2–5	1	3	0	0
S7	1.0	1.0	0.5–1.5	0.5	0.4	0.3–0.7	1	1	1–1	1	1	1.0	1.0
S8	0.8	0.8	0.5–1.1	0.3	0.1	0.1–0.5	1	1	1–1	1	1	0.3	0.3

Notes: “Age” means the age of the youngest stellar component. “ F_{b} ,” “ F_{r} ,” “ N_{sf} ” and “mod” mean binary fraction, rotating star fraction, number of star formation with interval of 0.1 Gyr, and star formation mode (1, 2 and 3 corresponds to homogeneous, linearly increasing and linearly decreasing modes with increasing age) respectively.

to find the best-fit model step by step. In detail, 51 simulated star clusters, including S1–S8, are used for testing the tool. Figure 5 displays the test results, in which the input and recovered values of seven parameters are compared. We find that distance modulus, color excess, metallicity, youngest-component age, age spread, binary fraction and rotating star fraction are recovered well. Note that age spread is described by another parameter, N_{sf} , which means the number of star formations from the youngest component and with an age interval of 0.1 Gyr. When checking the star formation mode, the input modes of 12 are recovered correctly, within 15 simulated star clusters. Therefore, *Powerful CMD* recovered the input parameters of most simulated star clusters. For the purpose of quantitative comparison, Tables 2 and 3 list the input and fitted parameters of eight simulated clusters (S1–S8).

5 APPLICATION TO FOUR STAR CLUSTERS

Four star clusters, i.e., NGC 6362, NGC 6652, NGC 6838 and M67, are used for testing the new tool. None of them have an obviously extended main-sequence turn off and therefore they can be fitted via SSPs. Readers can check our previous paper, Li et al. (2015), for a detailed study of the CMD of NGC 1651, which presents an extended main-sequence turn off. There have been some studies about these clusters being tested, and this enables us to compare our results

with previous results. The data on M67 are directly taken from Yadav et al. (2008). Those on the three other clusters (i.e., NGC 6362, NGC 6652 and NGC 6838) are obtained from the *HST* archive, which were observed with the Wide Field and Planetary Camera 2 (WFPC2) between 1996 and 2000. Images were obtained using the F439W (B) and F555W (V) filters. The exposure times of clusters NGC 6362, NGC 6652 and NGC 6838 in the F439W filter are 100, 100 and 160 s, and those in F555W filter are 40, 30 and 50 s, respectively. We handle the *HST* data using the stellar photometry package of Dolphin (2000) (HSTphot), because this package is specially designed for dealing with *HST* WFPC2 images and it has been widely used. Finally, we obtain the observed CMDs in the B and V bands for three clusters. The *HST* magnitudes are transformed to the B and V magnitudes by HSTphot. Following some previous works, e.g., Rubele et al. (2010), magnitude uncertainties are estimated via an AST technique, and the results are shown in Figure 6. Then Figure 7 shows the observed CMDs (black points). We can clearly see the evolutionary structures, including main sequence, main-sequence turn off, Hertzsprung gap and red giants. Such CMDs are ideal for CMD studies.

When we use *Powerful CMD* to fit the CMDs of four clusters, all observed CMDs are reproduced well. The best-fit CMDs (red points) are compared to the observed ones via Figure 7. The results from stellar population models without binaries are the same as those with

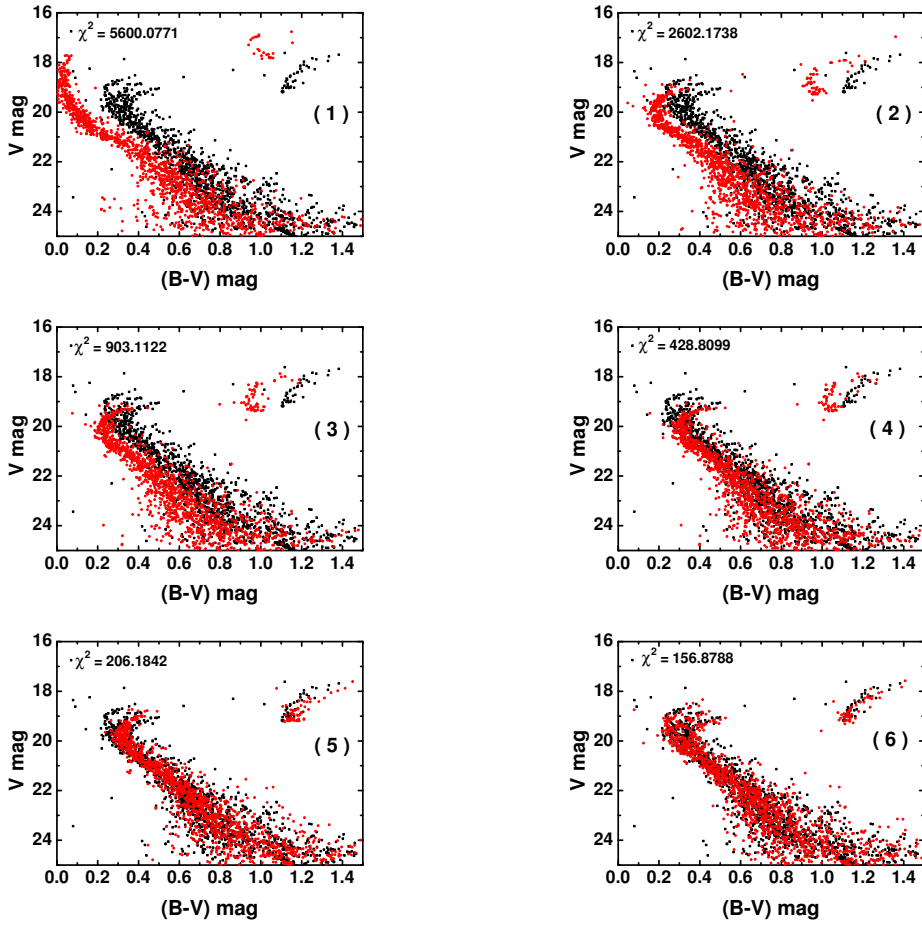


Fig. 4 Process illustrating the use of *Powerful CMD* to find the best-fit stellar population models. Black and red points are for observed and fitted CMDs, respectively. The less the χ^2 is, the better the goodness of fit. χ^2 less than 431 denotes acceptable models.

Table 4 Best-fit Parameters of Star Clusters NGC 6362, NGC 6652, NGC 6838 and M67 from SSP Models, Together with other Results

Cluster	$(m - M)$ [mag]	$(m - M)'$ [mag]	$E(B - V)$ [mag]	$E(B - V)'$ [mag]	Z	Z'	Age [Gyr]	Age' [Gyr]	F_b	Reference
NGC 6362	14.41	14.79	0.01	0.08	0.004	0.0020, 0.0024	13.2	13.57	0.8	Piotto, Forbes
NGC 6652	15.13	15.19	0.04	0.09	0.008	0.0021, 0.0022	12.8	12.93	0.8	Piotto, Forbes
NGC 6838	14.22	13.75	0.20	0.25	0.004	0.0037	13.4	13.70	0.6	Piotto, Forbes
M67	9.23	9.56–9.72	0.10	0.041	0.020	0.0209–0.0219	3.6	3.5–4.8	0.3	Yadav

Notes: A prime marker (') signifies results from other works (see reference). Binary fractions F_b are for all binaries with orbital period less than 100 yr, rather than interacting binaries.

binaries, except for color excess. The best-fit parameters are listed in Table 4 while 1σ ranges are in Table 5. “SSP-fit” and “CSP-fit” denote the results from SSP and CSP models, respectively. Note that in the fitting for M67, magnitude uncertainties are not considered as there are no available data. Because some other works have studied these clusters, we compare our results with others in Table 4. “Piotto,” “Forbes” and “Yadav” in Table 4 refer to the works of Piotto et al. (2002), Forbes & Bridges

(2010) and Yadav et al. (2008), respectively. Most of our results are consistent with previous works, although different stellar population models and fitting methods have been used. In detail, the $(m - M)$ and age values obtained in this work are similar to other works, with only a small difference (<0.5 mag and 0.4 Gyr). The metallicities of NGC 6838 and M67 agree well with previous works. Although there are differences for the metallicities of NGC 6362 and NGC 6652, they are actually lim-

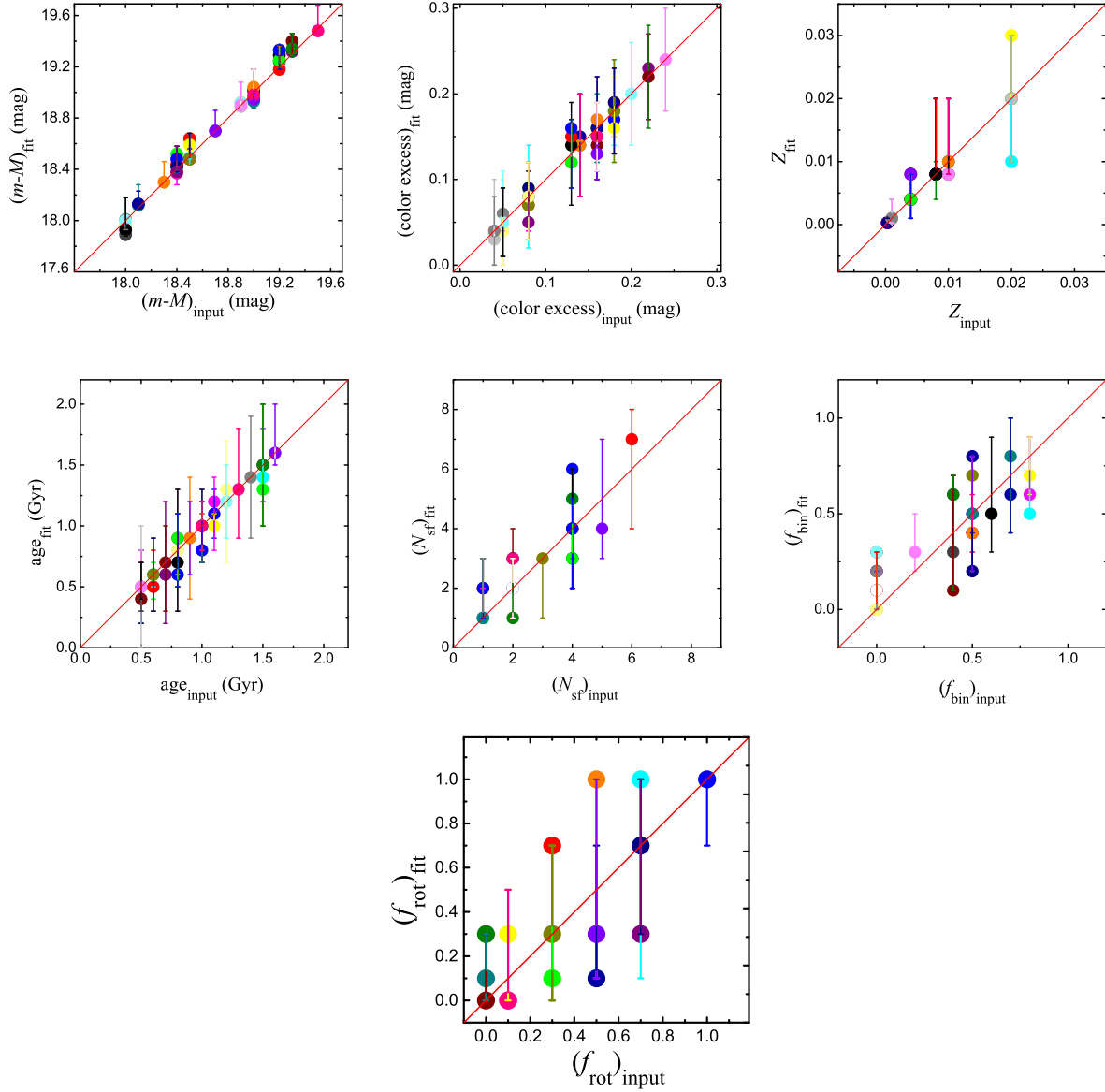


Fig. 5 Comparison of input and fitted parameters of 51 simulated star clusters. N_{sf} , f_{bin} and f_{rot} denote number of star bursts with an interval of 0.1 Gyr, binary fraction and rotating star fraction respectively. Error bars indicate 1σ uncertainties.

Table 5 Ranges of SSP-fit Parameters for Star Clusters NGC 6362, NGC 6652, NGC 6838 and M67 (The ranges correspond to 1σ confidence)

Cluster	$(m - M)$ range [mag]	$E(B - V)$ range [mag]	Z range	Age range [Gyr]	F_b range
NGC 6362	14.32–14.59	0.01–0.04	0.004	13.2–14.3	0.5–1.0
NGC 6652	15.00–15.40	0.01–0.08	0.008–0.010	11.8–13.8	0.6–0.9
NGC 6838	12.99–14.29	0.16–0.24	0.004	12.4–14.4	0.4–0.8
M67	9.03–9.62	0.07–0.19	0.010–0.030	3.1–4.1	0.2–0.4

Table 6 Best-fit Parameters of Star Clusters NGC 6362, NGC 6652 and NGC 6838 from CSP Models

Cluster	$(m - M)$ [mag]	$E(B - V)$ [mag]	Z	Age [Gyr]	F_b	Star formation mode
NGC 6362	14.42	0.02	0.004	13.0–13.5	0.7	decreasing
NGC 6652	14.94	0.03	0.008	12.6–12.7	0.7	homogeneous
NGC 6838	14.13	0.21	0.004	13.1–13.5	0.5	homogeneous

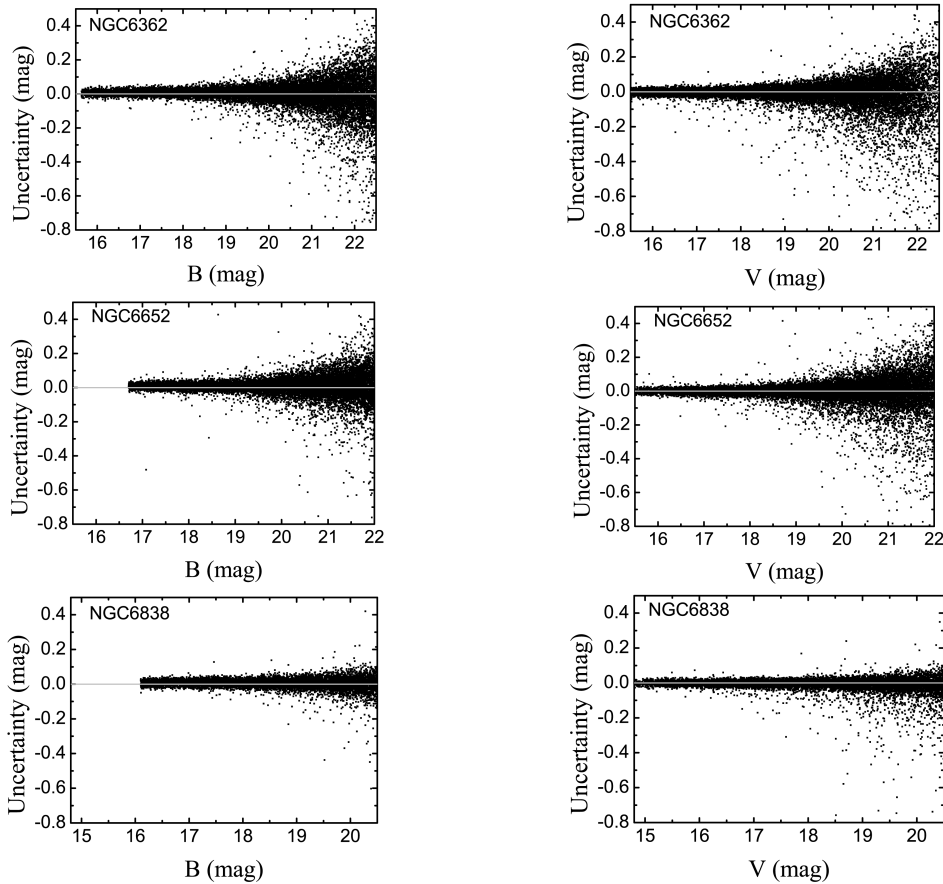


Fig. 6 Magnitude uncertainty as a function of magnitude for clusters NGC 6362, NGC 6652 and NGC 6838.

ited by the small number (eight) of metallicities used in theoretical stellar populations. If more metallicities are taken for theoretical populations, the results will be possibly closer. Moreover, we find that *Powerful CMD* reports smaller color excesses than previous results for all clusters. This is reasonable, because binaries are taken into account by this work. Some unresolved binaries are located to the right of the main sequence, and this makes it able to fit the observed CMDs with smaller color excesses. We can see that a high binary fraction (0.8) is determined for NGC 6362 and NGC 6652. This result is not unusual, because binaries here mean those with orbital periods less than 100 yr at the zero age, rather than interacting binaries or main sequence binaries with a large (>0.5) mass ratio.

In other words, binaries in this paper include all kinds of binaries. The binary components can be any type of star, including a black hole. Thereby, the binary fractions derived by *Powerful CMD* usually seem larger than in other works, e.g., Milone et al. (2012). The effects of binaries are studied widely, e.g., Li & Han (2009); Yang et al. (2011); Jiang et al. (2014). In addi-

tion, *Powerful CMD* reports an obviously smaller distance modulus for M67 compared to the previous result. This is also caused by the inclusion of binaries. As we see in the last panel of Figure 7, binaries enable us to fit the right part below turn-off with a smaller distance modulus compared to the case of single-star populations.

In the above test, we assume that these clusters are SSPs, because their CMDs seem similar to the isochrones of SSPs. However, some of them are possibly CSPs, which was suggested by e.g., Piotto et al. (2015); Milone et al. (2017). We therefore study the CMDs of star clusters NGC 6362, NGC 6652 and NGC 6838 using CSP models. We finally conclude that CSPs can fit the CMDs of three clusters better than SSPs.

Figure 8 compares the observed and best-fit models for two clusters and Table 6 shows the best-fit results of three clusters. We find that CSP models (Table 6) lead to smaller binary fractions compared to SSP models (Table 4), but other parameters are similar. The result is reasonable because both multiple populations and stellar binarity contribute to stars in the region outlined by the blue box (Fig. 8). In this case, the presence of mul-

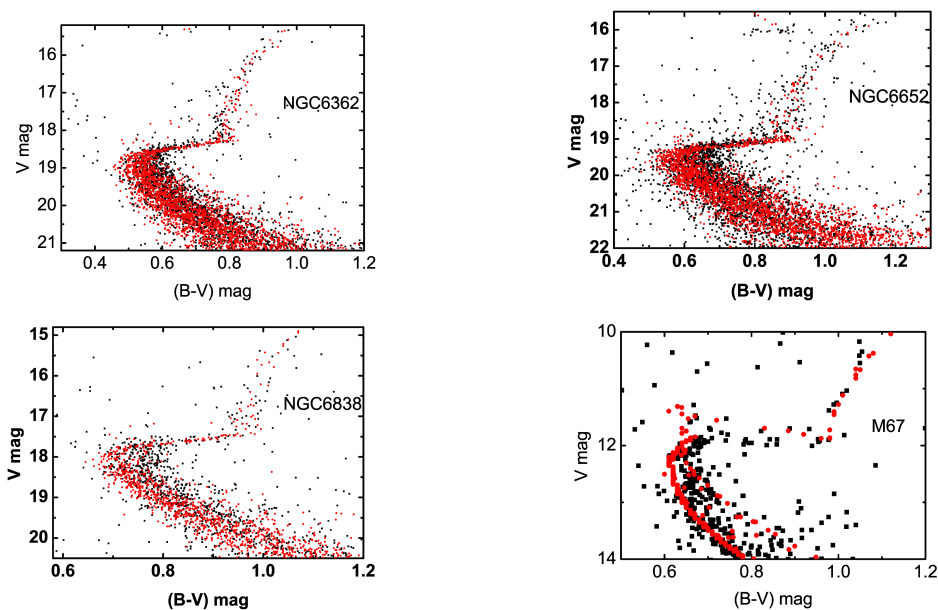


Fig. 7 Comparison of observed (*black*) and SSP-fit (*red*) CMDs of clusters NGC 6362, NGC 6652, NGC 6838 and M67. The observational uncertainties in magnitudes of M67 have not been considered.

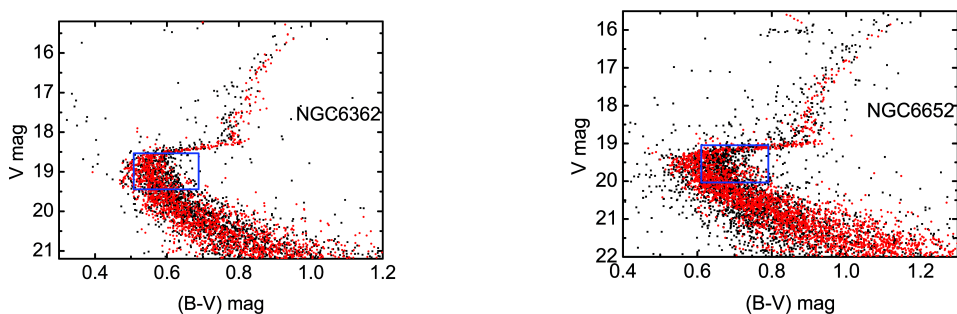


Fig. 8 Comparison of observed (*black*) and CSP-fit (*red*) CMDs of clusters NGC 6362 and NGC 6652. Blue boxes show the regions that CSP models can reproduce better than SSP models.

multiple populations in star clusters affects the result from *Powerful CMD*.

6 DISCUSSION AND CONCLUSIONS

We present a new tool for CMD studies, *Powerful CMD*, in this paper. The new tool can be used for building theoretical CMDs of various kinds of stellar populations, and for determining eight parameters of star clusters from CMDs. The relevant stellar population synthesis model (i.e., ASPs), building technique of synthetic CMDs and CMD fitting method were introduced first. Then we used *Powerful CMD* to build the CMDs of some artificial star clusters, and check the efficiency of *Powerful CMD* using these simulated CMDs. It is shown that the new tool has the ability to determine cluster parameters correctly. Finally, the new tool was applied to four star clusters to determine their distance moduli, color excesses, metal-

licities, ages and binary fractions. The observed CMDs were fitted well, and the best-fit parameters agree with previous works as a whole, although the inclusion of binaries in theoretical stellar population models leads to less color excesses for three clusters. This implies that *Powerful CMD* is a reliable tool for most CMD studies, in particular for the studies with *HST* CMDs.

A limitation of the current version of *Powerful CMD* is that the star formation mode of about 20% of star clusters cannot be automatically determined well. This is caused by the degeneracy of different parameters. *Powerful CMD* has supplied a function to determine the detailed star formation histories when other parameters are known. If we can determine the stellar population types (SSP or CSP) via other methods, e.g., spectra, *Powerful CMD* will be able to determine the star formation histories. In addition, this tool still contains some

uncertainties, which may result from uncertainties in the modeling of stellar evolution (including single stars, binaries and rotators), assumptions about stellar properties (e.g., IMF, distributions of binary separation and eccentricity, and distribution of stellar rotation rates), estimation of observational uncertainties, and statistics for CMD fitting. We will study them more thoroughly in the future and improve the code.

Moreover, *Powerful CMD* utilizes a large amount of data. This aspect makes it not easy to disseminate this tool. The authors will be glad to provide it to all astronomers for free in the future. Meanwhile, we are trying to make the tool and data available to the public as soon as possible.

Acknowledgements We thank the referee for useful comments. This work is supported by the National Natural Science Foundation of China (Grant Nos. 11563002 and 11373003), the Joint Research Project of Sino-German Center (GZ1284), the National Key Basic Research Program of China (973 Program No. 2015CB857002) and Yunnan Science Foundation (project name “*Study of Binary Fraction of Star Clusters*”). We thank Prof. Li Chen of Shanghai Astronomical Observatory for suggestions.

References

- Anderson, J., Sarajedini, A., Bedin, L. R., et al. 2008, *AJ*, 135, 2055
- Bertelli, G., Nasi, E., Girardi, L., et al. 2003, *AJ*, 125, 770
- Brandt, T. D., & Huang, C. X. 2015, *ApJ*, 807, 25
- Cignoni, M., & Shore, S. N. 2006, *A&A*, 454, 511
- Da Rio, N., Gouliermis, D. A., & Gennaro, M. 2010, *ApJ*, 723, 166
- D’Antona, F., Di Criscienzo, M., Decressin, T., et al. 2015, *MNRAS*, 453, 2637
- De Gennaro, S., von Hippel, T., Jefferys, W. H., et al. 2009, *ApJ*, 696, 12
- Dolphin, A. E. 2000, *PASP*, 112, 1383
- Dolphin, A. E. 2002, *MNRAS*, 332, 91
- Forbes, D. A., & Bridges, T. 2010, *MNRAS*, 404, 1203
- Fusi Pecci, F., Buonanno, R., Cacciari, C., et al. 1996, *AJ*, 112, 1461
- Georgy, C., Ekström, S., Granada, A., et al. 2013, *A&A*, 553, A24
- Harris, J., & Zaritsky, D. 2001, *ApJS*, 136, 25
- Hurley, J. R., Tout, C. A., & Pols, O. R. 2002, *MNRAS*, 329, 897
- Hurley, J., & Tout, C. A. 1998, *MNRAS*, 300, 977
- Jiang, D., Han, Z., & Li, L. 2014, *ApJ*, 789, 88
- Kerber, L. O., & Santiago, B. X. 2005, *A&A*, 435, 77
- Kerber, L. O., Santiago, B. X., Castro, R., & Valls-Gabaud, D. 2002, *A&A*, 390, 121
- Li, Z., & Han, Z. 2008a, *MNRAS*, 387, 105
- Li, Z., & Han, Z. 2008b, *ApJ*, 685, 225
- Li, Z.-M., & Han, Z.-W. 2009, *RAA (Research in Astronomy and Astrophysics)*, 9, 191
- Li, Z.-M., Mao, C.-Y., Li, R.-H., Li, R.-X., & Li, M.-C. 2010, *RAA (Research in Astronomy and Astrophysics)*, 10, 135
- Li, Z. 2011, in *Astronomical Society of the Pacific Conference Series*, 451, 9th Pacific Rim Conference on Stellar Astrophysics, eds. S. Qain, K. Leung, L. Zhu, & S. Kwok, 51
- Li, Z., Mao, C., Chen, L., & Zhang, Q. 2012a, *ApJ*, 761, L22
- Li, Z., Zhang, L., & Liu, J. 2012b, *MNRAS*, 424, 874
- Li, Z., Mao, C., Chen, L., Zhang, Q., & Li, M. 2013, *ApJ*, 776, 37
- Li, Z., Mao, C., & Chen, L. 2015, *ApJ*, 802, 44
- Li, Z., Mao, C., Zhang, L., Zhang, X., & Chen, L. 2016, *ApJS*, 225, 7
- Mackey, A. D., & Broby Nielsen, P. 2007, *MNRAS*, 379, 151
- Mackey, A. D., Broby Nielsen, P., Ferguson, A. M. N., & Richardson, J. C. 2008, *ApJ*, 681, L17
- Mieske, S., Jordán, A., Côté, P., et al. 2006, *ApJ*, 653, 193
- Milone, A. P., Stetson, P. B., Piotto, G., et al. 2009, *A&A*, 503, 755
- Milone, A. P., Piotto, G., Bedin, L. R., et al. 2012, *A&A*, 540, A16
- Milone, A. P., Piotto, G., Renzini, A., et al. 2017, *MNRAS*, 464, 3636
- Naylor, T., & Jeffries, R. D. 2006, *MNRAS*, 373, 1251
- Niederhofer, F., Bastian, N., Kozhurina-Platais, V., et al. 2016, *A&A*, 586, A148
- Niederhofer, F., Georgy, C., Bastian, N., & Ekström, S. 2015, *MNRAS*, 453, 2070
- Olsen, K. A. G., Hodge, P. W., Mateo, M., et al. 1998, *MNRAS*, 300, 665
- Piotto, G., King, I. R., Djorgovski, S. G., et al. 2002, *A&A*, 391, 945
- Piotto, G., Milone, A. P., Bedin, L. R., et al. 2015, *AJ*, 149, 91
- Royer, F., Zorec, J., & Gómez, A. E. 2007, *A&A*, 463, 671
- Rubele, S., Kerber, L., & Girardi, L. 2010, *MNRAS*, 403, 1156
- Salpeter, E. E. 1955, *ApJ*, 121, 161
- Sandquist, E. L., Bolte, M., Stetson, P. B., & Hesser, J. E. 1996, *ApJ*, 470, 910
- VandenBerg, D. A., Brogaard, K., Leaman, R., & Casagrande, L. 2013, *ApJ*, 775, 134
- von Hippel, T., Jefferys, W. H., Scott, J., et al. 2006, *ApJ*, 645, 1436
- Yadav, R. K. S., Bedin, L. R., Piotto, G., et al. 2008, *A&A*, 484, 609
- Yang, W., Bi, S., Meng, X., & Liu, Z. 2013, *ApJ*, 776, 112
- Yang, W., Meng, X., Bi, S., et al. 2011, *ApJ*, 731, L37